Widely Linear Beamforming for Full-Duplex Joint Communications and Sensing: an Investigation on Virtual Displacement of Array Elements during Local Optimization

Hadi Alidoustaghdam*, Yang Miao and André Kokkeler
Radio systems group, University of Twente
Enschede, the Netherlands
✉ *: *hadi.alidoustaghdam@utwente.nl*

***Abstract*—In this paper, we have a closer look at widely linear beamforming (WLB) for full-duplex Joint Communication and Sensing (JCAS). WLB is a powerful method for mitigating the effect of IQ imbalances in array radiation. In full-duplex JCAS, the transmitting aperture radiates multi-beams focusing towards the communication user and the sensing target, while simultaneously the receiving aperture receives sensing signals. When applying WLB intended for interference mitigation between the transmitting and receiving apertures, mirror beams often occur and degrade the mitigation effect.**

In this paper, we propose to use virtual displacement of array elements during local optimization in WLB to further reduce the mirror beams. The virtual displacement is to deviate the antenna elements virtually in WLB optimization process and, in the numerical analysis, we show that this can be a solution for interference mitigation while we use uniform arrays in practice. This approach can facilitate the usage of modular hardware for JCAS.

***Index Terms*—6G, joint communication and sensing, interference mitigation.**

I. Introduction

Joint communication and sensing (JCAS) is a key feature for 6G, and is expected to achieve both high data rates and high-resolution sensing simultaneously [1], [2]. Integrating sensing and communication functionality in assembled multi-input multi-output (MIMO) systems requires innovative solutions. When the same array of antennas is employed as both the transmit and receive aperture via switching and time division, the current state-of-art electronics and also the communication frames are usually so long that pulse radar operation is impossible [3]. Alternatively, one can segment the array into transmit and receive apertures operating simultaneously: the transmit aperture forms separate beams for communicating to the user and sensing the dynamics in the environment; the receive aperture receives sensing signals [3], [4]. Such full-duplex operation of transmitting and receiving beams could suffer from the mutual interference between the two, and thus proper interference mitigation is crucial.

As one approach to mitigate the interference between the transmit and receive beams, the authors in [3] have investigated linear beamforming for the uniform linear arrays. Adopting a local optimization approach, the beamforming weights of the antennas for the transmit aperture are calculated first; then the weights for the receive aperture are calculated by the combination of a null-space projection (NSP) matrix and a matched filter. Consequently, mirror beams occur due to the lack of phase variations for the weights of the receive aperture. To this end, in [3], some antenna elements are displaced to randomize the coupling of transmitter and receiver apertures and obtain a final design of an array configuration that suffers from the least damage caused by mirror beams. Displaced array elements make the manufacturing of arrays difficult; besides, since this method is based on linear beamforming, the performance is deteriorated in case of in-phase quadrature-phase (IQ) imbalances. Beyond [3], this paper considers IQ imbalances in the apertures and the constraint of manufacturing, by adopting widely linear beamforming (WLB) [5] and incorporating virtual array displacements only in the optimization/processing phase, to mitigate IQ imbalances, interference and mirror beams. Instead of beamforming on uniform arrays, the beamforming is applied on the displaced virtual arrays

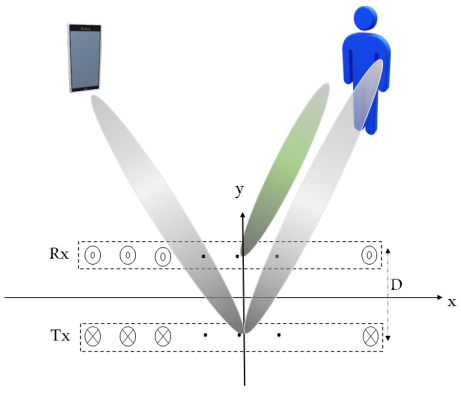

Fig. 1. A simplified JCAS scenario enabled by a co-located array: transmit aperture with two beams focusing toward the communication user and the sensing target; receive aperture for signals impinging from the sensing target.

which does not suffer from mirror beams, the migration from the response of the uniform array to virtual arrays is based on spatial interpolation.

II. Formulation of Problem

A. Widely linear beamforming

We formulate a simplified JCAS scenario with one communication user and one sensing entity, as is shown in Fig. 1. A co-located, linear array comprises a transmit (Tx) and a receive (Rx) aperture with N_t and N_r antennas respectively; the two sets of apertures are separated by a distance of $\mathbf{D}$. In case of IQ imbalances in the Rx aperture, the output signal of receiver without noise, denoted by $\tilde{y}_{\text{RX,imb}}$, can be written as [5]:

$$\begin{aligned}\tilde{y}_{\text{RX,imb}} = (\mathbf{W}_{1r}^H\mathbf{K}_{1r} + \mathbf{W}_{2r}^H\mathbf{K}_{2r}^*)\mathbf{x} + ... \\ (\mathbf{W}_{1r}^H\mathbf{K}_{2r} + \mathbf{W}_{2r}^H\mathbf{K}_{1r}^*)\mathbf{x}^*,\end{aligned} \tag{1}$$

where $\mathbf{W}_{1r} \in \mathbb{C}^{N_r\times 1}$ and $\mathrm{W}_{2r} \in \mathbb{C}^{N_r\times 1}$ are two weight vectors, $\mathbf{K}_{1r} \in \mathbb{C}^{N_r\times N_r}$ and $\mathbf{K}_{2r} \in \mathbb{C}^{N_r\times N_r}$ are the known matrices attributed to the IQ imbalances. $\mathbf{x} \in \mathbb{C}^{N_r\times 1}$ is a vector containing the signals at the output of each Rx antenna. $()^*$ and $()^H$ are the complex conjugate and Hermitian operators, respectively. When we consider Tx and Rx apertures in proximity (i.e. $\mathbf{D}$ in Fig. 1 is approximately equal to half wavelength), the contribution of mutual coupling to interference needs to be mitigated. The signal after WLB at Tx would be:

$$\begin{aligned}\tilde{\mathbf{x}}_{\text{TX,imb}} = (\mathbf{W}_{1t}^H\mathbf{K}_{1t} + \mathbf{W}_{2t}^H\mathbf{K}_{2t}^*)x + ... \\ (\mathbf{W}_{1t}^H\mathbf{K}_{2t} + \mathbf{W}_{2t}^H\mathbf{K}_{1t}^*)x^*,\end{aligned} \tag{2}$$

where x is the baseband signal snapshot for transmission and $\tilde{\mathbf{x}}_{\text{TX,imb}} \in \mathbb{C}^{1\times N_t}$ is a vector containing the signal snapshots at each Tx antenna element, $\mathbf{W}_{1t} \in \mathbb{C}^{N_t\times 1}$ and $\mathbf{W}_{2t} \in \mathbb{C}^{N_t\times 1}$ are the weights for WLB, $\mathbf{K}_{1t} \in \mathbb{C}^{N_t\times N_t}$ and $\mathbf{K}_{2t} \in \mathbb{C}^{N_t\times N_t}$ denote the IQ imablances of the Tx aperture. The interference matrix representing inherent mutual coupling among antenna elements, denoted by $\mathbf{H}_{\text{SI}}(f) \in \mathbb{C}^{N_r\times N_t}$, is frequency dependent and can be measured or estimated via EM simulator. If we consider $\mathbf{x} = \mathbf{H}_{\mathbf{SI}}\tilde{\mathbf{x}}_{\text{TX,imb}}^T$ as the signal vector which is coupled from Tx to Rx aperture, and substitute it into (1), the interference when both apertures are excited by their weights can be thus calculated. This interference depends on the random variable x and its power can be written as:

$$\begin{aligned}&P_{int} = \sigma_x^2 \times \Big(\\ &\Big|(\mathbf{W}_{1r}^H\mathbf{K}_{1r} + \mathbf{W}_{2r}^H\mathbf{K}_{2r}^*)\mathbf{H}_{\text{SI}}(\mathbf{W}_{1t}^H\mathbf{K}_{1t} + \mathbf{W}_{2t}^H\mathbf{K}_{2t}^*)^T + \\ &(\mathbf{W}_{1r}^H\mathbf{K}_{2r} + \mathbf{W}_{2r}^H\mathbf{K}_{1r}^*)\mathbf{H}_{\text{SI}}^*(\mathbf{W}_{1t}^H\mathbf{K}_{2t} + \mathbf{W}_{2t}^H\mathbf{K}_{1t}^*)^H\Big|^2 + \\ &\Big|(\mathbf{W}_{1r}^H\mathrm{K}_{1r} + \mathrm{W}_{2r}^H\mathbf{K}_{2r}^*)\mathbf{H}_{\text{SI}}(\mathbf{W}_{1t}^H\mathbf{K}_{2t} + \mathbf{W}_{2t}^H\mathbf{K}_{1t}^*)^T + \\ &(\mathbf{W}_{1r}^H\mathbf{K}_{2r} + \mathbf{W}_{2r}^H\mathbf{K}_{1r}^*)\mathbf{H}_{\text{SI}}^*(\mathbf{W}_{1t}^H\mathbf{K}_{1t} + \mathbf{W}_{2t}^H\mathbf{K}_{2t}^*)^H\Big|^2\Big),\end{aligned} \tag{3}$$

where $()^T$ is the transpose operator, and it is assumed that x has no self-correlation $\mathbb{E}[xx] = 0$, $\sigma_x^2 = \mathbb{E}[|x|^2]$ is the signal power and equal to unit here.

Now let us write the radiation patterns for Tx and Rx apertures. In WLB [5], the mirror beam due to IQ imbalances in Tx aperture can be mitigated by:

$$\begin{aligned}\mathbf{W}_{1t}^H\mathbf{K}_{1t} + \mathbf{W}_{2t}^H\mathbf{K}_{2t}^* = \mathbf{W}_{tx}^H \\ \mathbf{W}_{1t}^H\mathbf{K}_{2t} + \mathbf{W}_{2t}^H\mathbf{K}_{1t}^* = \mathbf{0}_{N_t}\end{aligned} \tag{4}$$

where:

$$\mathbf{W}_{tx} = \frac{\sqrt{\rho}\mathbf{a}_t(\theta_c) + \sqrt{1-\rho}\mathbf{a}_t(\theta_r)}{\left\|\sqrt{\rho}\mathbf{a}_t(\theta_c) + \sqrt{1-\rho}\mathbf{a}_t(\theta_r)\right\|} \tag{5}$$

and $\mathbf{a}_t(\theta) \in \mathbb{C}^{N_t\times 1}$ is the narrowband beam steering vector of Tx aperture:

$$\mathbf{a}_t(\theta) = \begin{bmatrix} e^{jk(x_{1,t}\cos\theta + y_{1,t}\sin\theta)} \\ \vdots \\ e^{jk(x_{N_t,t}\cos\theta + y_{N_t,t}\sin\theta)}\end{bmatrix} \tag{6}$$

where θ is the angle measured from z axis, $x_{i,t}$ and $y_{i,t}$ denote the coordinate of ith antennas and k is the wave-number. θ_c and θ_r are angles toward the communication user and the sensing target respectively, $0 < \rho < 1$ is the parameter controlling the power allocated to the communication and sensing beams, which is chosen to be 0.5 here. $\mathbf{0}_{N_t}$ is a vector with N_t zeros. $\mathbf{W}_{1t}$ and $\mathbf{W}_{2t}$ can be calculated by (4), then the power of the radiation pattern for Tx aperture is:

$$\tilde{D}_{\text{TX,imb}}(\theta) = |\mathbf{W}_{1t}^H\mathbf{K}_{1t}\mathbf{a}_t(\theta) + \mathbf{W}_{2t}^H\mathbf{K}_{2t}^*\mathbf{a}_t(\theta)|^2 \tag{7}$$

By substituting (4) into (3), we have:

$$\begin{aligned}&P_{int} = \\ &\Big|(\mathbf{W}_{1r}^H\mathbf{K}_{1r} + \mathbf{W}_{2r}^H\mathbf{K}_{2r}^*)\mathbf{H}_{\text{SI}}(\mathbf{W}_{1t}^H\mathbf{K}_{1t} + \mathbf{W}_{2t}^H\mathbf{K}_{2t}^*)^T\Big|^2 + \\ &\Big|(\mathbf{W}_{1r}^H\mathbf{K}_{2r} + \mathbf{W}_{2r}^H\mathbf{K}_{1r}^*)\mathbf{H}_{\text{SI}}(\mathbf{W}_{1t}^H\mathbf{K}_{1t} + \mathbf{W}_{2t}^H\mathbf{K}_{2t}^*)^T\Big|^2\end{aligned} \tag{8}$$

For $P_{int} = 0$, we can write for the weights in the Rx aperture according to null-space projection matrix and WLB [3]:

$$\begin{aligned}\mathbf{W}_{1r}^H\mathbf{K}_{1r} + \mathbf{W}_{2r}^H\mathbf{K}_{2r}^* = \frac{\left((\mathbf{I} - \mathbf{F}\mathbf{F}^\dagger)\mathbf{a}_r(\theta_r)\right)^*}{\left\|(\mathbf{I} - \mathbf{F}\mathbf{F}^\dagger)\mathbf{a}_r(\theta_r)\right\|} \\ \mathbf{W}_{1r}^H\mathbf{K}_{2r} + \mathbf{W}_{2r}^H\mathbf{K}_{1r}^* = \mathbf{0}_{N_r}\end{aligned} \tag{9}$$

where $\mathbf{F} = \mathbf{H}_{\text{SI}}(\mathbf{W}_{1t}^H\mathbf{K}_{1t} + \mathbf{W}_{2t}^H\mathbf{K}_{2t}^*)^T$ and $\mathbf{F}^\dagger$ is its pseudo-inverse. When $\mathbf{W}_{1r}$ and $\mathbf{W}_{2r}$ are calculated based on (9), the radiation pattern for the Rx aperture would be:

$$\tilde{D}_{\text{RX,imb}}(\theta) = |\mathbf{W}_{1r}^H\mathbf{K}_{1r}\mathbf{a}_r(\theta) + \mathbf{W}_{2r}^H\mathbf{K}_{2r}^*\mathbf{a}_r(\theta)|^2 \tag{10}$$

As it will be shown by the numerical results, although (9) satisfies $P_{int} = 0$, when $\theta_c = -\theta_r$ or $\theta_r = 0$, a mirror beam appears due to the angle of the communication user in the Rx radiation pattern as in [3]. Instead of fully relying on WLB, we intend to add some phase changes to the weights of Tx and Rx apertures to investigate the behavior of Tx, Rx patterns and interference levels. The phase changes are modeled by virtual displacement of antennas from a uniform array.

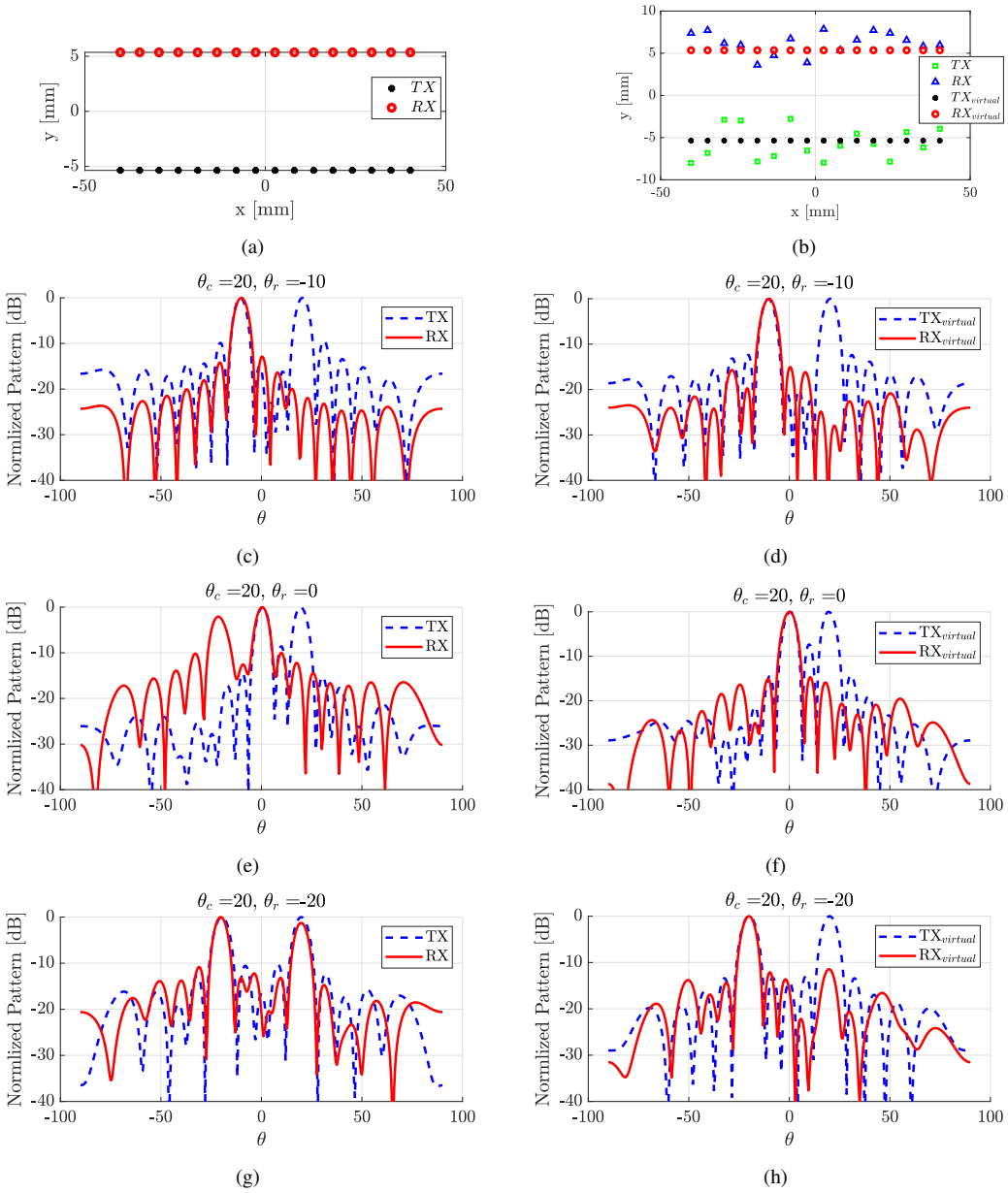

Fig. 2. (a) The geometry of uniform linear Tx and Rx apertures, (b) a demonstration of virtual displacement of elements of Tx and Rx apertures in WLB optimization; the normalized patterns for (c) uniform linear arrays when $\theta_c = +20^o$, $\theta_r = -10^o$ and $P_{int} = -39$ dB (d) virtual arrays when $\theta_c = +20^o$, $\theta_r = -10^o$ and $P_{int} = -38.9$ dB, (e) uniform linear arrays when $\theta_c = +20^o$, $\theta_r = 0^o$ and $P_{int} = -41$ dB (f) virtual arrays when $\theta_c = +20^o$, $\theta_r = 0^o$ and $P_{int} = -22.49$ dB, (g) uniform linear arrays when $\theta_c = +20^o$, $\theta_r = -20^o$ and $P_{int} = -62$ dB (h) virtual arrays when $\theta_c = +20^o$, $\theta_r = -20^o$ and $P_{int} = -24$ dB.

B. Virtual Array

Assuming the antennas are displaced from their positions in linear arrays, the new weights of Tx and Rx apertures change, based on WLB. We also calculate a new mutual coupling matrix for such displaced arrays as follows. If we consider Fig. 1 as a multi-static antenna array, the system's response can be expressed as a vector $\mathbf{S} = [s_{11}, s_{12}, s_{13}, ..., s_{N_t N_r}]^T \in \mathbb{C}^{N_t N_r \times 1}$. It is intended to obtain a relationship between s and the locations of transmit and receive antennas as in [6]:

$$s(\vec{r_t}, \vec{r_r}) = w_0 + \sum_{i=t,r} w_i \vec{r_i} + \sum_{i=t,r} \sum_{j=t,r} w_{ij} \vec{r_i} \vec{r_j} + e \quad (11)$$

where w are the unknown coefficients, $\vec{r_t}$ and $\vec{r_r}$ are the locations of transmit and receive antennas. Thus (11) can be written in a matrix form as:

$$\mathbf{S} = \mathbf{R}\mathbf{w} + \mathbf{e} \quad (12)$$

where $\mathbf{R} = [\mathbf{r}(r_1), \mathbf{r}(r_2), ..., \mathbf{r}(r_{N_t N_r})]^T \in \mathbb{R}^{N_t N_r \times 7}$ is the location's quadratic function matrix, where $\mathbf{r}(r_i) =$

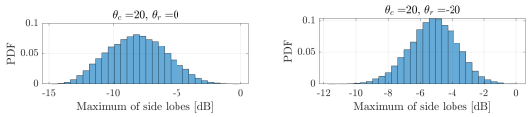

(a) (b)

Fig. 3. The PDFs for the maximum value of side lobes in the pattern of Rx aperture for (a) $\theta_c = +20^o$ and $\theta_r = 0^o$, (b) $\theta_c = +20^o$ and $\theta_r = -20^o$.

$[1, \vec{r}_{t_i}, \vec{r}_{r_i}, \vec{r}^2_{t_i}, \vec{r}_{t_i}\vec{r}_{r_i}, \vec{r}_{r_i}\vec{r}_{t_i}, \vec{r}^2_{r_i}]^T$ and $\mathbf{e} \in \mathbb{C}^{N_t N_r \times 1}$ is the error vector. The best linear unbiased estimation of $\mathbf{w} \in \mathbb{C}^{7\times 1}$ by the Kriging method [7] is:

$$\hat{\mathbf{w}} = (\mathrm{R}^T\mathbf{C}^{-1}\mathbf{R})^{-1}\mathbf{R}^T\mathbf{C}^{-1}\mathbf{S} \tag{13}$$

where $\mathbf{C} = [c_{ij}]$ is the $N_tN_r \times N_tN_r$ correlation matrix. For simplicity, only the phase change of electromagnetic waves are considered and a farfield model as in [6] is used:

$$c_{ij} = e^{-ik|r_i - r_j|} \tag{14}$$

where r_i and r_j are the distances between transmitter and receiver for the ith and jth transmitter-receiver pairs, respectively. Once $\hat{\mathbf{w}}$ is calculated, we can obtain the multi-static response of virtual arrays system $\hat{\mathbf{S}}(\mathbf{r}_v)$ as:

$$\hat{\mathbf{S}}(\mathbf{r}_v) = \mathbf{r}(\mathbf{r}_v)\hat{\mathbf{w}} + \mathbf{c}(\mathbf{r}_v)^T\mathbf{C}^{-1}(\mathbf{S} - \mathbf{R}\hat{\mathbf{w}}) \tag{15}$$

where $\mathbf{r}_v$ denotes the locations of virtual transmitter-receiver pairs and $\mathbf{c}(\mathbf{r}_v)$ is the correlation matrix between the location of virtual transmitter-receiver pairs with the location of uniform linear arrays. As $\mathbf{c}(\mathbf{r}_v)$ is calculated based on (14) which is a farfield modelling, the mutual impedance should not have drastic change for the virtual displacements from physical Tx, Rx apertures. The $\hat{\mathbf{S}}(\mathbf{r}_v)$ will be the new coupling matrix $\mathbf{H}_{\mathrm{SI}}$ used in (9) and the virtual arrays will be used for Tx and Rx beamforming. When the weights are calculated, they are finally applied on the original uniform array for obtaining the new patterns and interference.

III. Numerical Analysis

Let us follow the scenario in Fig. 1 with two uniform linear arrays as TX and RX apertures. In the numerical example, we employed rectangular patch antennas with patch sizes of $l_x \times l_y = 3.9 \times 2.73$ mm^2 on the Rogers RO3003 substrate with thickness 0.25 mm, relative permittivity of $\epsilon_r = 3$ and copper cladding thickness of 35 μm. These antenna are designed for a working central frequency of $f_0 = 28$ GHz, bandwidth $\mathrm{BW}_{10\text{ dB}} = 863$ MHz and half-power beamwidth of $89.3^\circ < \theta_{3\text{ dB}} < 119.1^\circ$ for various ϕs. The number of antennas is $N_t = 16$ and $N_r = 16$ for Tx and Rx apertures, respectively, with inter-element spacing of $\lambda_0/2$ where λ_0 is the wavelength at central frequency f_0. Since only the phase change is considered for different transmitter-receiver pairs in (14), the magnitude of the mutual impedance should not change drastically when there are small, virtual translation displacement of the elements. Therefore, the virtual displacement has to be in the vicinity of uniform linear arrays. Besides, the magnitude of mutual impedance of two patch antennas does not have large variations when the inter-distance ranges from $0.75\lambda_0$ to $1.25\lambda_0$ [8]; therefore, we chose D in Fig. 1 equal to λ_0 and also the deviations from uniform arrays are considered only for the y-axis and generated for $-\lambda_0/4 < \delta_y < \lambda_0/4$ with a uniform random distribution. CST studio is used to simulate the mutual impedance of the uniform linear Tx, Rx apertures at the frequency of $f_0 = 28$ GHz and mutual coupling matrix $\mathbf{H}_{\mathrm{SI}}(f_0)$ is calculated based on the Z-parameters. Then, the mutual coupling matrix for displaced arrays is obtained based on mutual coupling of uniform arrays and the method in II.B. The matrices $\mathbf{K}_1$ and $\mathbf{K}_2$ in (7) and (9) are generated by a uniform random distribution in $0.75 < g < 1.25$ and $-15^o < \phi < +15^o$ for the relative gain and phase mismatches in the Tx, Rx chains as in [5].

Let us first demonstrate the performance of uniform linear Tx and Rx arrays where $\theta_c = 20^o$ and $\theta_r = -10^o$. It is shown in Fig. 2 (c) that the Tx pattern has two beams towards the communication user and sensing target whereas the Rx aperture has a single beam toward the sensing target. When the sensing target moves to $\theta_r = 0^o$ or $\theta_r = -20^o$, a mirror beam appears at $-\theta_c$ as in Fig. 2 (e) and (g).

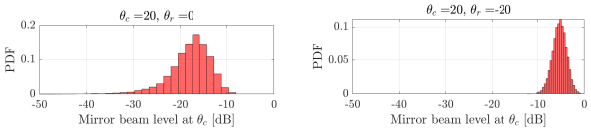

(a) (b)

Fig. 4. The PDFs for the value of mirror beam in the pattern of Rx aperture for (a) $\theta_c = +20^o$ and $\theta_r = 0^o$, (b) $\theta_c = +20^o$ and $\theta_r = -20^o$.

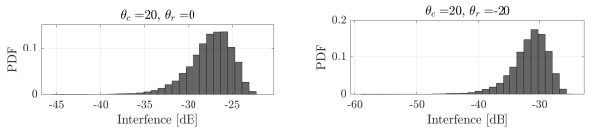

(a) (b)

Fig. 5. Interference level from Tx to Rx aperture when (a) $\theta_c = +20^o$ and $\theta_r = 0^o$, (b) $\theta_c = +20^o$ and $\theta_r = -20^o$.

Let us now consider incorporating virtual displacement only in the optimization, as proposed in Sec. II B. A randomized version of uniform Tx and Rx apertures is shown in Fig. 2 (c). As it is shown in Figs. 2 (f) and (h), the mirror beams due to the communication user are disappeared and the level of intererference is increased to -20 dB. Although one can record this geometry of virtual displacement of arrays to use in practice; however, as this geometry is generated randomly only in the processing phase, we can also apply a Monte Carlo simulation to study the maximum of side lobes and the mirror beam in the pattern of virtual Rx aperture. Probability distribution functions (PDF) for the value of maximum side lobes and mirror beam in the pattern of virtual Rx aperture are obtained by 20000 simulations. As shown in Fig. 3 (a) and (b), the level of side lobes are suppressed, besides the mean of power for the mirror beam is -17 dB as in Fig. 4 (a) and -5dB

in Fig. 4 (b). The level of interference is almost -28 dB as in Fig. 5 (a) and (b). Therefore, complementary interference mitigation is still necessary for full-duplex operation.

IV. Conclusion

Joint Communication and Sensing (JCAS) calls for powerful signal processing algorithms to enable multi-beams fulfilling both requirements of communication and sensing. We proposed to use widely linear beamforming and virtual displacement of array elements in the optimization process to mitigate interference between the simultaneous transmitting multi-beams and receiving beam while guaranteeing the desired radiation patterns. Through numerical analysis, it is shown that, in the presence of IQ imbalances, the proposed approach can result in -20 dB interference, although complimentary interference mitigation will be needed. Compared to the recent literature, using virtual displacements rather than the actual design of the irregular arrays, makes the implementation of JCAS hardware more flexible.

References

[1] T. Wild, V. Braun, and H. Viswanathan, "Joint design of communication and sensing for beyond 5g and 6g systems," *IEEE Access*, vol. 9, pp. 30 845–30 857, 2021.

[2] C. De Lima, D. Belot, R. Berkvens, A. Bourdoux, D. Dardari, M. Guillaud, M. Isomursu, E.-S. Lohan, Y. Miao, A. N. Barreto *et al.*, "Convergent communication, sensing and localization in 6g systems: An overview of technologies, opportunities and challenges," *IEEE Access*, 2021.

[3] M. Heino, C. B. Barneto, T. Riihonen, and M. Valkama, "Design of phased array architectures for full-duplex joint communications and sensing," in *2021 15th European Conference on Antennas and Propagation (EuCAP)*. IEEE, 2021, pp. 1–5.

[4] C. Baquero Barneto, T. Riihonen, S. Damith Liyanaarachchi, M. Heino, N. González-Prelcic, and M. Valkama, "Beamformer design and optimization for full-duplex joint communication and sensing at mm-waves," *arXiv e-prints*, pp. arXiv–2109, 2021.

[5] A. Hakkarainen, J. Werner, K. R. Dandekar, and M. Valkama, "Widely-linear beamforming and rf impairment suppression in massive antenna arrays," *Journal of Communications and Networks*, vol. 15, no. 4, pp. 383–397, 2013.

[6] A. Zamani, A. M. Abbosh, and S. Crozier, "Multistatic biomedical microwave imaging using spatial interpolator for extended virtual antenna array," *IEEE Transactions on Antennas and Propagation*, vol. 65, no. 3, pp. 1121–1130, 2017.

[7] J. P. Kleijnen, "Kriging metamodeling in simulation: A review," *European journal of operational research*, vol. 192, no. 3, pp. 707–716, 2009.

[8] D. R. Jackson, W. F. Richards, and A. Ali-Khan, "Series expansions for the mutual coupling in microstrip patch arrays," *IEEE transactions on antennas and propagation*, vol. 37, no. 3, pp. 269–274, 1989.